ARCHIVES of FOUNDRY ENGINEERING

ISSN (1897-3310)
Volume 10
Issue 1/2010

109 – 114

21/1

Published quarterly as the organ of the Foundry Commission of the Polish Academy of Sciences

Bainite obtaining in cast iron with carbides castings

S. Pietrowski, G. Gumienny*
Department of Materials Technologies and Production Systems, Technical University of Łódź,
Stefanowskiego 1/15 Street, 90-924 Łódź, Poland
* Corresponding author: E-mail address: grzegorz.gumienny@p.lodz.pl

Received 14.07.2009; accepted in revised form 22.07.2009

Abstract

In these paper the possibility of upper and lower bainite obtaining in cast iron with carbides castings are presented. Conditions, when in cast iron with carbides castings during continuous free air cooling austenite transformation to upper bainite or its mixture with lower bainte proceeds, have been given. A mechanism of this transformation has been given, Si, Ni, Mn and Mo distribution in the eutectic cell has been tested and hardness of tested castings has been determined.

Keywords: Innovative Foundry Technologies and Materials, Nodular Cast Iron with Carbides, Bainite, TDA Method

1. Introduction

Upper, lower bainite or its mixture as-cast obtaining in cast iron encounters difficulties, so in practice most often heat treatment is used. Thereupon, in the Department of Materials Technologies and Production Systems of Technical University of Łódź research work obtaining upper and lower bainite or its mixture in the metal matrix of nodular cast iron with carbides are conducted. Preliminary findings are presented in work [1]. The aim of this work was to investigate the possibility of upper and lower bainite or its mixture obtaining as-cast in nodular cast iron castings with use of Inmold technology and to give the mechanism of the bainitic transformation.

2. Work methodology

Cast iron was melted in 30kg induction furnace of 15000Hz frequency. To cast iron melting Norwegian pig iron OB and St3 steel scrap were used. Silicon content was supplemented by FeSi75 ferrosilicon and manganese – FeMn65 ferromanganese. To cast iron modification "Inmold" method was used. A master alloy in amounts of 1% casting mass was located in the reactive chamber in the gating system. After this chamber the mixing and the control chamber were located. Inside the control chamber the thermoelement PtRh10-Pt (S type) was placed. The thermoelement through compensatory conductors was connected with the Cristaldigraph to thermal derivative analysis (TDA) curves recording. Investigations were executed on samples Y shape and 25mm wall thickness. After the crystallization finish castings were knocking out and free air cooling. The chemical composition of tested cast iron, its equivalent carbon content E_c and a degree of eutectic saturation S_c are presented in Table 1.

Table 1.
The chemical composition of tested cast iron, its equivalent carbon content E_c and a degree of eutectic saturation S_c

Chemical composition, %								E_c, %	S_c
C	Si	Mn	Mo	Ni	P_{max}	S_{max}	Mg		
3,57 ÷ 3,66	2,48 ÷ 2,54	0,19 ÷ 0,22	1,00 ÷ 2,00	0,00 ÷ 1,00	0,05	0,01	0,05	4,37 ÷ 4,41	1,02 ÷ 1,03

Cast iron microstructure was tested on metallographic specimens nital etched, magn. ×1000 on the metallographic microscope and ×5000 on the S-3000N Hitachi scanning microscope. Hardness tests were made by use of HPO hardness testing machine with conditions: 2,5/187,5/30. X-ray microanalysis was made by using Pioneer ESD detector and Ventago software.

3. Results

In Figure 1 (a, b) representative TDA curves of nodular cast iron (a) and its microstructure (b) are presented.

a)

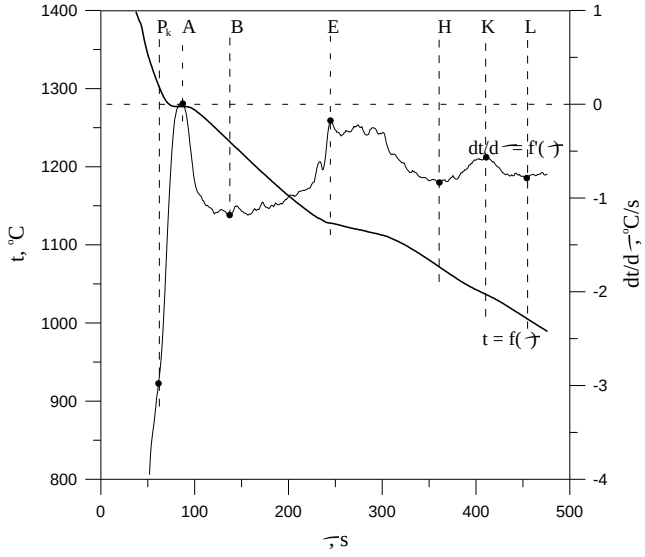

Point	τ, s	t, °C	dt/dτ, °C/s
P_k	61	1305	-2,97
A	87	1277	0,01
B	137	1232	-1,18
E	245	1128	-0,17
H	361	1072	-0,84
K	411	1036	-0,57
L	454	1006	-0,79

b)

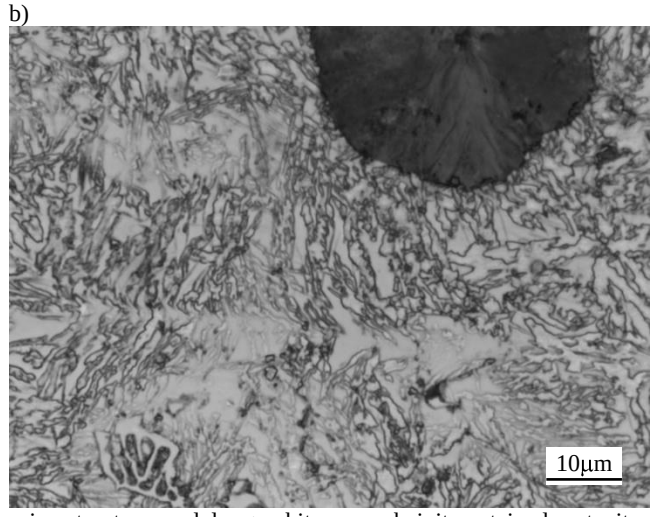

microstructure: nodular graphite, upper bainite, retained austenite, ledeburitic carbides

Fig. 1 (a, b). TDA curves (a) and the microstructure (b) of nodular cast iron containing: 3,60% C, 2,50% Si, 0,20% Mn, 2,00% Mo, 0,50% Ni (E_c = 4,37%)

Cast iron has got the microstructure consisting of: nodular graphite, upper bainite, retained austenite, ledeburitic carbides. It has hypereutectic composition (E_c = 4,37%). Thereupon cast iron crystallization starts from the graphite precipitation, what causes on the derivative curve P_kAB thermal effect. BEH thermal effect comes from the graphite eutectic crystallization. With regard to Mo occurrence in cast iron, which is characterized by straight microsegregation, its elements are "pushing down" deep into the liquid. Thereupon, from tH = 1072°C residual liquid cast iron crystallizes according to the metastable system and $(Fe,Mo)_3C$ ledeburitic carbides are formed. They are located on eutectic cells boundaries. In Figure 2 (a, b) the metal matrix microstructure of cast iron near to the graphite (a) and near to the eutectic cell boundary (b) are presented.

a)

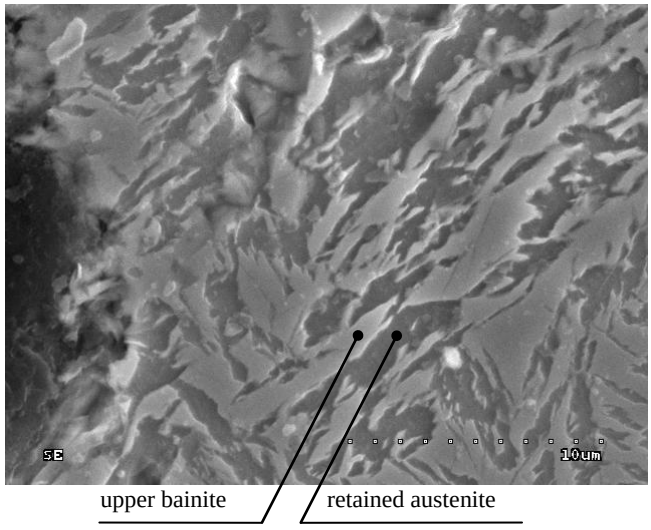

b)

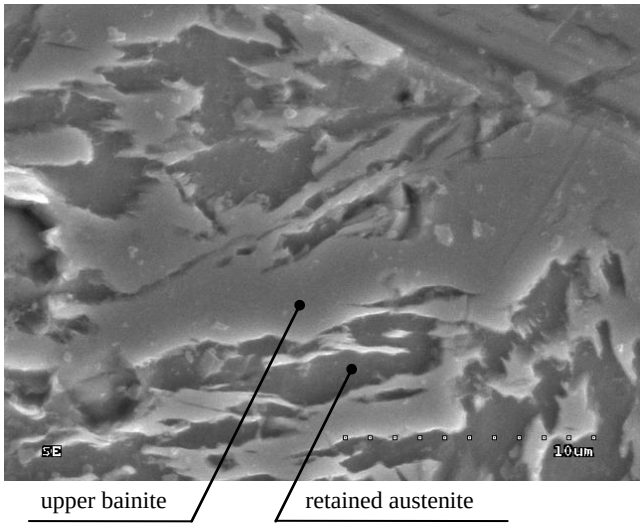

Fig. 2 (a, b). The metal matrix microstructure of cast iron near to the graphite (a) and near to the eutectic cell boundary (b). Scanning, magn. ×5000

Results from it significant diversification of upper bainite plates size inside the eutectic cell. The average size of upper bainite plates created near to the graphite is smaller than plates located near to the eutectic cell boundary. In Fig. 1b it is shown a bainite size reduction near to ledeburitic carbide, too. Results from it, that $\gamma \rightarrow B_G$ transformation starts on graphite/austenite and carbide/austenite boundaries. There is a small amount of carbon and molybdenum in these micro-areas, so the austenite stability is the least. Through supersaturation of bainitic ferrite by carbon, the diffusion of its elements to cell boundaries begins, where carbides precipitate. They form together with the ferrite an upper bainite. Precipitated carbides are probably Mo enriched. $\gamma \rightarrow B_G$ transformation on eutectic cells starts later. Thereupon, precipitated upper bainite plates are bigger and more expanded (Fig. 2b). $\gamma \rightarrow B_G$ transformation scheme is shown in Figure 3.

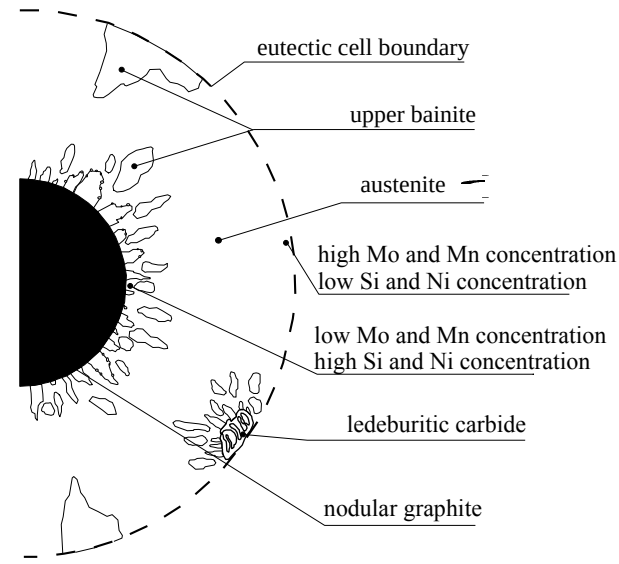

Fig. 3. $\gamma \rightarrow B_G$ transformation scheme in the eutectic cell of nodular cast iron with carbides

There is a different character of the austenite transformation in cast iron, which TDA curves and the microstructure are presented in Figure 4 (a, b).

a)

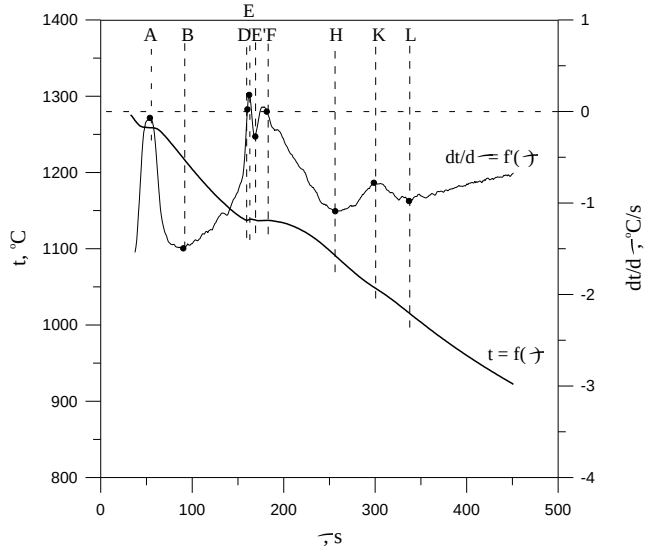

Point	τ, s	t, °C	dt/dτ, °C/s
A	54	1259	-0,07
B	90	1219	-1,50
D	160	1137	–
E	162	1138	0,18
E‘	169	1138	-0,27
F	181	1137	–
H	256	1091	-1,09
K	299	1050	-0,78
L	337	1016	-0,98

b)

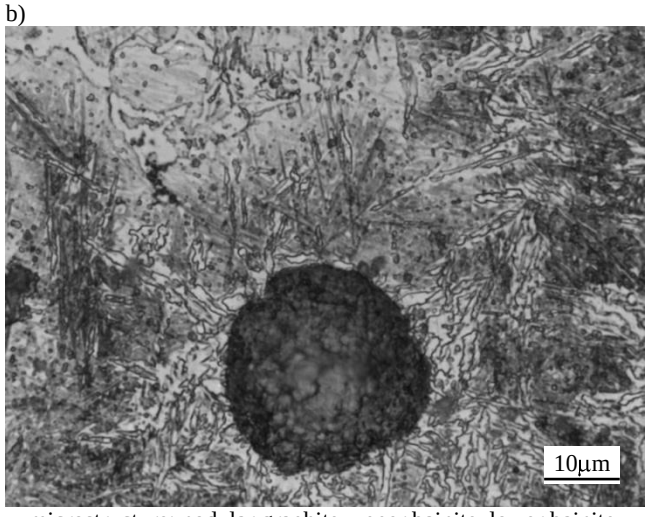

microstructure: nodular graphite, upper bainite, lower bainite, retained austenite, primary carbides

Fig. 4 (a, b). Representative TDA curves (a) and the microstructure of nodular cast iron containing: (b): 3,60% C, 2,50% Si, 0,20% Mn, 2,00% Mo, 1,00% Ni (E_c = 4,39%)

This cast iron, in comparison with the previous, has got increased nickel concentration to 1,00%. From TDA curves results, that cast iron crystallization starts from primary graphite precipitation (AB thermal effect). BDEE' thermal effect comes from primary carbides precipitation and E'FH – from graphite eutectic. Probably primary carbides form due to increased nickel concentration. Similarly like in previous cast iron, after γ + graphite eutectic crystallization finish, cast iron starts its crystallization according to the metastable system. Thereupon $(Fe,Mo)_3C$ ledeburitic carbides are formed in tH = 1091°C ÷ tL = 1016°C (HKL thermal effect, Fig. 4a). They are exemplary shown in Figure 5. Cast iron metal matrix microstructure is the mixture of upper and lower bainite. $\gamma \rightarrow B_G + B_D$ transformation starts from upper bainite plates formation. Start of $\gamma \rightarrow B_G$ transformation takes place near to the graphite and carbides (Fig. 4b). An austenite surrounding upper bainite is supersaturated by carbon and during later cooling on the boundary with upper bainite, lower bainite plates increase. $\gamma \rightarrow B_D$ transformation is preceded by upper bainite precipitations. On the γ/B_G interfacial boundary the transformation to lower bainite starts. Thereupon, a lower bainite is surrounded from all directions by upper bainite, like it is shown in Figure 6 (a, b).

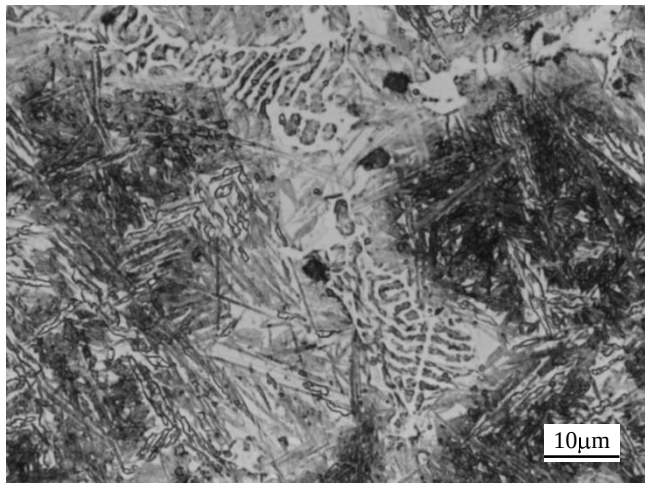

Fig. 5. Ledeburitic carbides in the upper and lower bainite matrix in nodular cast iron

a)

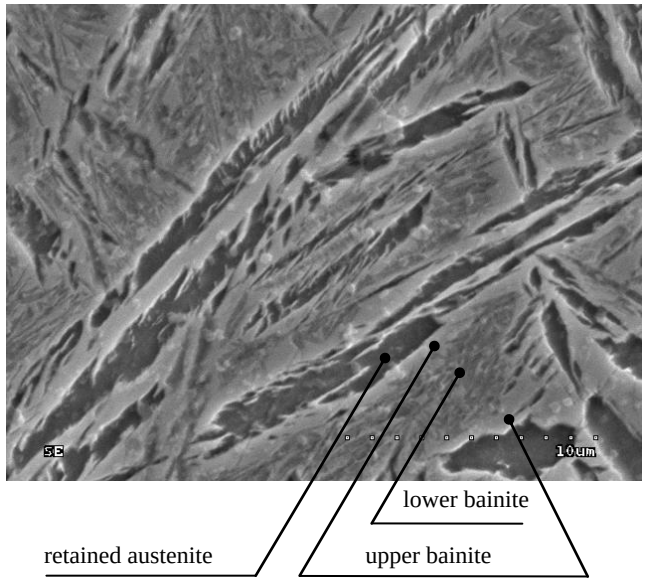

b)

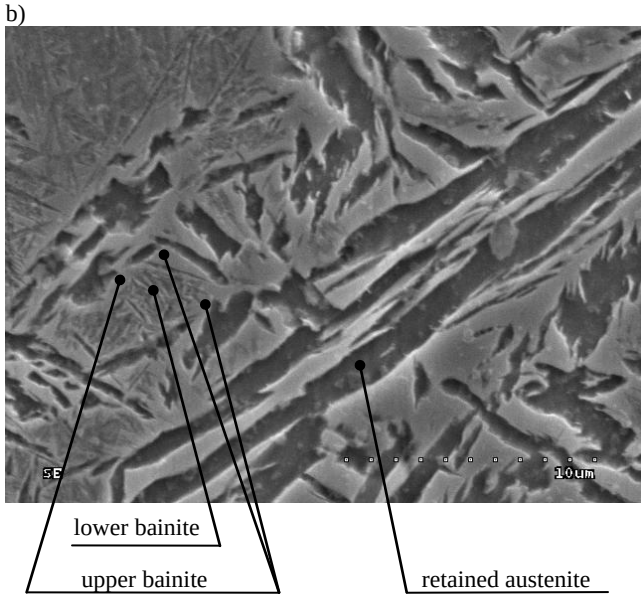

Fig. 6 (a, b). The microstructure of metal matrix near to the graphite (a) and near to the eutectic cell boundary (b) of nodular cast iron. Scanning, magn. ×5000

Results from it a greater size reduction of upper and lower bainite near to the graphite in comparison with the area near to the eutectic cell boundary. It confirm the fact of austenite transformation start to upper bainite on the graphite/austenite interfacial boundary. Near to upper bainite, a fine lower bainite increases. Upper bainite and its mixture with lower bainite forming is schematically presented on TTT curves in Figure 7.

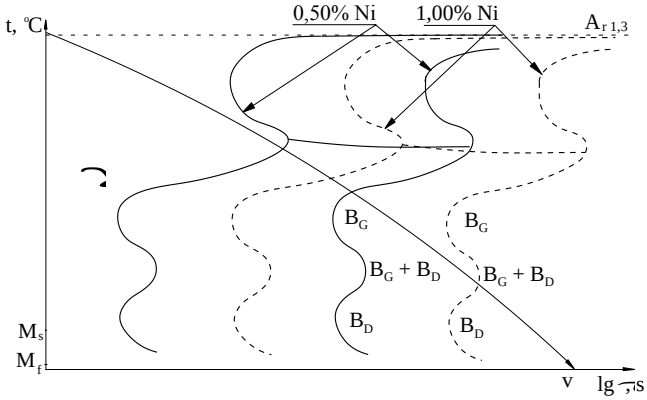

Fig. 7. The scheme of upper bainite and its mixture with lower bainite obtaining in nodular cast iron with carbides

TTT curves of nodular cast iron containing 0,50% and 1,00% Ni are presented on it. In both cases there was Mo in amounts of 2,00%. Start of austenite decomposition in cast iron containing 1,00% Ni is displaced to longer time. For the identically cooling rate in cast iron containing 0,50% of Ni there is only $\gamma \rightarrow B_G$ transformation, while in cast iron containing 1,00% of Ni $\gamma \rightarrow B_G + B_D$ transformation takes place.

Studies of Si, Ni, Mn and Mo concentration distribution in the eutectic cell have been conducted. The representative distribution of these elements with the measuring length is presented in Figure 8 (a ÷ e).

a)

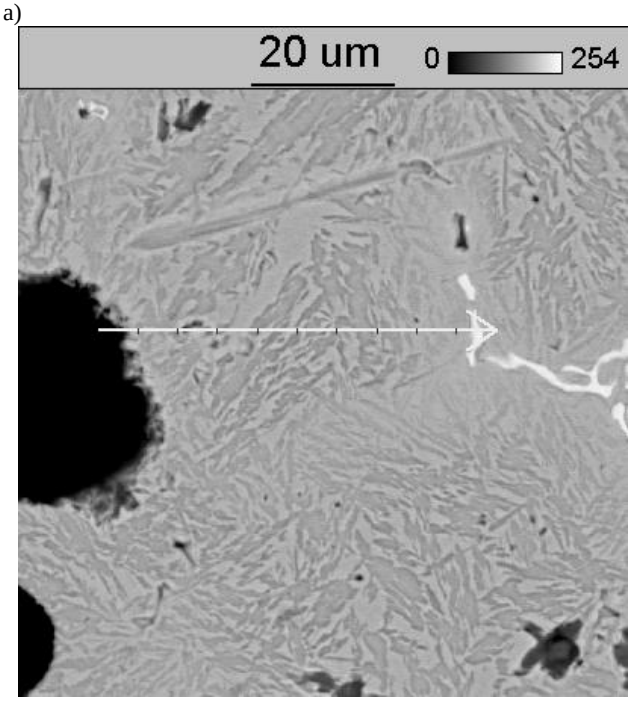

b)

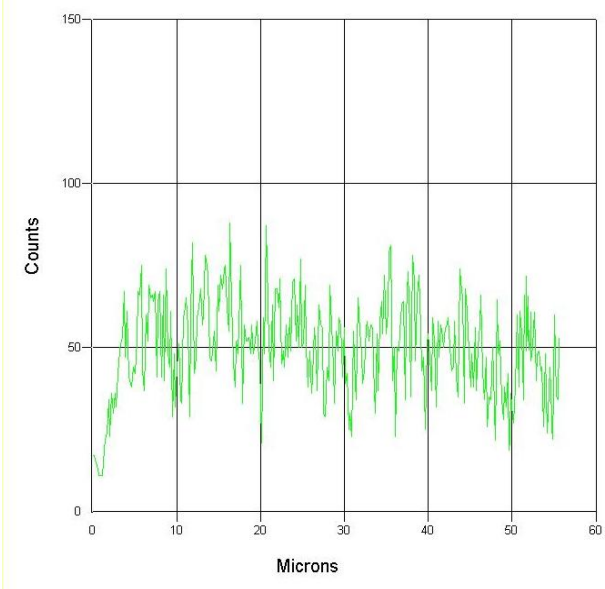

c)

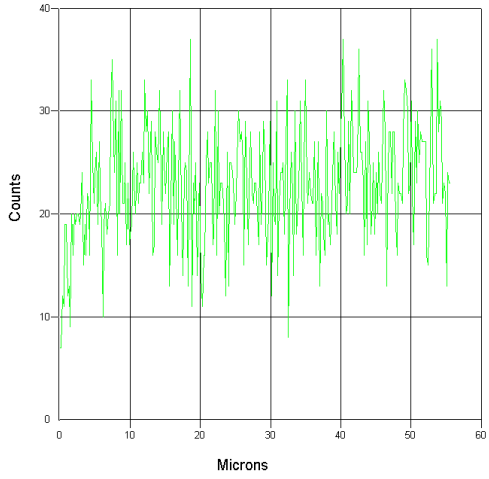

d)

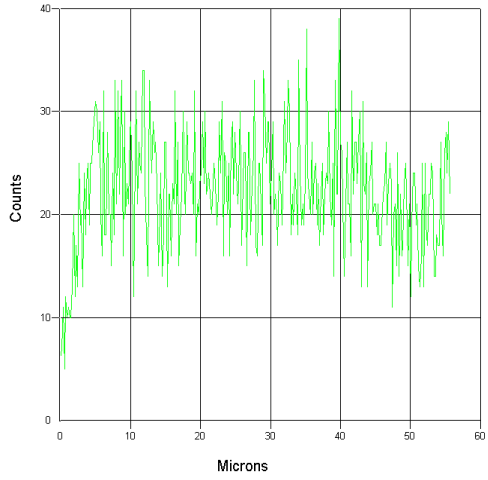

e)

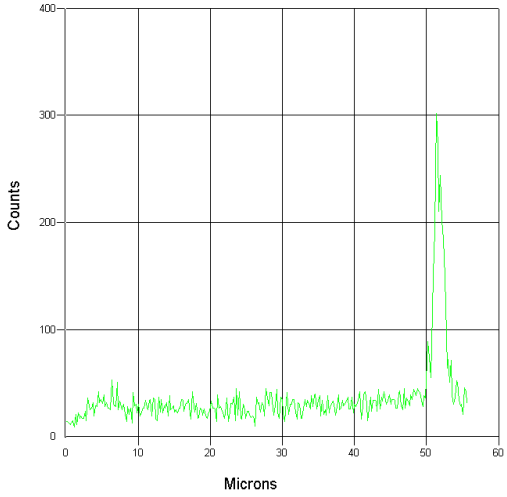

Fig. 8 (a ÷ e). The microstructure and the measuring length (a) and the linear distribution of: Si (b), Mn (c), Ni (d) and Mo (e) in the eutectic cell

Results from it, that Si and Ni are characterized by inverse microsegregation, i.e. near to the graphite their concentration is a bit greater than near to the eutectic cell. Manganese has insignificantly increased concentration near to the eutectic cell. From Fig. 8e results a great Mo concentration in the carbide and slight concentration in cast iron metal matrix.

The average hardness of nodular cast iron with carbides and upper bainite had 312HB and cast iron with upper and lower bainite mixture – 417HB.

4. Conclusions

The results have indicated the following:

- $\gamma \rightarrow B_G$ transformation starts from graphite/austenite and carbide/austenite interfacial boundaries,
- in cast iron with 2,00% Mo and 0,50% Ni free air cooling it is possible to obtain as-cast upper bainite microstructure,
- an increase of Ni concentration to 1,00% causes upper and lower bainite mixture obtaining in cast iron,
- $\gamma \rightarrow B_G + B_D$ transformation is preceded by $\gamma \rightarrow B_G$ transformation,
- after austenite transformation finish lower bainite is surrounded from all directions by upper bainite.

References

[1] G. Gumienny, Bainitic nodular cast iron with carbides obtaining with use of Inmold method, Archives of Foundry Engineering, 2009 vol. 9, Issue 3, s. 243-248.

[2] S. Pietrowski, The influence of the chemical composition of nodular cast steel and cast iron and casting cooling rate on the austenite transformation to acicular structures, Scientific Books No 94, Łódź 1987 (in Polish).

[3] S. Pietrowski, Bainitic ferrite with austenite or bainitic nodular cast iron, Archives of Materials Science, Vol. 18, No 4 (1997) 253-273 (in Polish).